Electronic Nature of the Transition State for Nucleoside Hydrolase. A Blueprint for Inhibitor Design†

Benjamin A. Horenstein and Vern L. Schramm*

Department of Biochemistry, Albert Einstein College of Medicine of Yeshiva University, 1300 Morris Park Avenue, Bronx, New York 10461

Received January 7, 1993; Revised Manuscript Received April 20, 1993

ABSTRACT: A new approach to understanding transition-state structure is presented which involves the sequential application of experimental and computational methods. A family of experimentally determined kinetic isotope effects is fit simultaneously in a vibrational analysis to provide a geometric model of the transition state. The electrostatic potential surface of the geometric model is defined by molecular orbital calculations to detail the electronic nature of the transition state. The method provides both geometric and charge information for the enzyme-stabilized transition state. Electrostatic potential surface calculations were applied to the *N*-glycohydrolase reaction catalyzed by nucleoside hydrolase from the trypanosome *Crithidia fasciculata*. A geometric model of the transition-state structure for the enzymatic hydrolysis of inosine by nucleoside hydrolase has been established by the analysis of a family of kinetic isotope effects [Horenstein, B. A., Parkin, D. W., Estupinan, B., & Schramm, V. L. (1991) *Biochemistry 30*, 10788]. The transition state has substantial oxycarbonium ion character, but the results of electrostatic potential calculations indicate that the transition-state charge is distributed over the ribosyl ring rather than existing as a localized $C^+—O \leftrightarrow C{=}O^+$ resonance pair. The electrostatic potential surfaces of the substrate and enzyme-bound products differ considerably from that of the transition state. At the transition state both hypoxanthine and ribose demonstrate regions of positive charge. The positive charge on the ribosyl oxycarbonium ion is moderated by association with an enzyme-directed water nucleophile. The enzyme-bound products contain adjacent areas of negative charge. The electrostatic potential surfaces provide novel insights into transition-state structure and the forces causing release of products. The reaction coordinate for nucleoside hydrolase can now be defined in terms of the molecular electrostatic potential surface of inosine as it traverses the reaction coordinate. Ribonolactone and 1,4-dideoxy-1,4-iminoribitol contain several geometric features of the transition state, respectively, and are superior inhibitors compared to substrate, substrate analogues, or products.

A variety of mechanisms have been suggested by which the activation energy for chemical reactions may be reduced in enzymic catalysis. Geometric, electronic, and covalent interactions with enzymes have been implicated (Jencks, 1969; Knowles, 1991; Hackney, 1990; Menger, 1992). A large portion of the rate acceleration is thought to reside in lowering the energy of the transition state for the reaction by selectively binding it, relative to the ground state. The observation that catalytic antibodies can be obtained by selection with transition-state analogue haptens provides the most recent evidence for transition-state stabilization [e.g., Lerner et al. (1991)]. A better understanding of transition-state structure is required for a deeper understanding of enzymatic catalysis. However, the fleeting lifetimes and low concentrations of transition states make their characterization challenging. Kinetic techniques, which report on the high-energy steps through the reaction coordinate, offer the only routine way to experimentally report on enzymatic transition-state structure. Kinetic isotope effects have thus proven to be an indispensable tool for describing the structural features of the transition state (Suhnel & Schowen, 1991; Huskey, 1991; Cleland, 1982). Isotope effects for specific transition states have been calculated using simple valence force field, semiempirical, and *ab initio* approaches using the rigid-rotor harmonic-oscillator approximation (Sims & Lewis, 1984; Brown et al., 1978; Saunders et al., 1989; Lu et al., 1990). The simple valence-force-field approach is advantageous in that it allows rapid modeling at points along an entire enzymatic reaction coordinate. The simple valence-force-field modeling approach treats a specific transition-state geometry as a stationary point on the reaction coordinate. *Ab initio* and semiempirical computational approaches seek to identify *the* minimum energy saddle point that exists on a given reaction coordinate energy surface. The simple valence-force-field approach is far less demanding computationally and allows evaluation of isotope effects for any proposed structure. Several chemical and enzymatic transition states have been modeled by vibrational analysis of experimental multiple kinetic isotope effects and, in some cases, provide detailed geometries for the transition states (McClennan, 1987; Mentch et al., 1987; Hermes et al., 1984; Rodgers et al., 1982; Markham et al., 1987; Parkin et al., 1991a; Horenstein et al., 1991).

With a defined transition-state geometry, the electronic features of a transition state may be determined. The high-energy bonding schemes of transition states are accompanied by altered distributions of electrons that reflect development of charge. Predictions of enzyme–transition state interactions and factors which stabilize the development of charge require the ability to describe molecular electronic properties of the transition state. An experimental approach to satisfy this requirement might employ Hammett relationships; however, this approach provides information only at the site of bond breaking (Hammett, 1970; Williams, 1992). We have

† This work was supported by Research Grants GM41916 and GM21083 from the NIH and Fellowship PF3298 from the American Cancer Society. The authors gratefully acknowledge a computational grant from the Pittsburgh Supercomputer Center.

* To whom correspondence should be addressed.

0006-2960/93/0432-7089$04.00/0

explored computational approaches to this problem using the well-defined transition state of nucleoside hydrolase (Horenstein et al., 1991).

Nucleoside hydrolase has been proposed to participate in purine salvage in the trypanosome *Crithidia fasciculata*. The enzyme hydrolyzes the N-glycosidic linkage of the naturally occurring purine and pyrimidine nucleosides. As this salvage pathway does not have a direct counterpart in mammalian metabolism, trypanosomal purine salvage enzymes are potential targets for the logical design of inhibitors (Parkin et al., 1991b; Perigaud et al., 1992). A geometric model of the transition state for nucleoside hydrolase has been described for the reaction:

$$\text{inosine} + H_2O \rightarrow \text{hypoxanthine} + \text{ribose}$$

The results of those studies indicated that there was substantial oxycarbonium ion character in the transition state, as evidenced by large 1′-α and 2′-β secondary tritium kinetic isotope effects measured with [1′-^{3}H]inosine and [2′-^{3}H]inosine, respectively (Horenstein et al., 1991). The 2′-^{3}H effect indicates the extent of oxycarbonium ion induced hyperconjugation in the ribose ring. The value of this isotope effect was larger for the enzymatic reaction than that observed for the acid-catalyzed hydrolysis of AMP (Parkin & Schramm, 1987). These isotope effects together with additional isotope effects using [1′-^{14}C]-inosine, [9-^{15}N]inosine, [4′-^{3}H]inosine, and [5′-^{3}H]inosine were analyzed by a bond-energy, bond-order vibrational analysis (Sims & Lewis, 1984) and used to construct the transition-state model of Figure 1 (Horenstein et al., 1991).

The present study is a departure from previous work by applying electrostatic potential calculations to transition-state structures on the basis of experimentally determined kinetic isotope effects. The *N*-glycosyl cationic transition state for nucleoside hydrolase is defined and compared to reactants and products. The distribution of electrostatic potential over the entire surface of the transition-state ensemble is described, as well as its relationship to the mechanism of the reaction and to the reaction coordinate. The influence of hydroxyl group rotomeric conformation at the transition state is explored as an example of structural information which is not available from the kinetic isotope effect experiments. Finally, the potential of the approach is demonstrated by observation of favorable interaction of ribonolactone and 1,4-dideoxy-1,4-iminoribitol with nucleoside hydrolase, compounds which contain several features of the transition state.

METHODS

Calculation of Atomic Charges. Net atomic charges were investigated as a method to describe the electronic properties of various species on the reaction coordinate. Mulliken and electrostatic-potential-derived semiempirical and *ab initio* molecular calculations were also investigated and compared (Frisch et al., 1992; Besler et al., 1990). Mulliken atomic charges assigned to *individual* atoms were dependent on the basis or parameter set employed and, in some cases, gave unusual and unexpected atomic charges. Mulliken charges divide the bonding-orbital overlap population equally between a bonding pair. The arbitrary partitioning of electron density in the Mulliken analysis can lead to unrealistic assignments of charge, especially in the unusual bonding patterns found at the transition state. More complex schemes to partition electron density in a physically realistic way have been suggested [e.g., Bader (1985)]. This problem can be partially relieved by summing charges over subregions of a molecule, but this approach did not provide sufficient resolution of charge properties for specific locations on the molecular species. Also, local charge was considered to be an essential feature when addressing enzyme–ligand interactions and designing transition-state analogue inhibitors. The extrapolation of atomic charges from the electrostatic potential necessarily condenses the large electrostatic potential data set to a small number of atomic charges. This procedure results in loss of information at the molecular surface, the critical region for understanding interactions between the enzyme and the transition state. A method was sought that would take advantage of current computational and graphical techniques to provide electronic information on the entire transition-state ensemble in a way that was physically intuitive. Molecular electrostatic potentials are well suited for this purpose.

Calculation of Molecular Electrostatic Potentials. The molecular electrostatic potential is widely used to describe electronic properties of molecules (Politzer & Truhlar, 1981). It is the difference in interaction energy for a point probe of unit charge between the nuclei and electrons at a defined distance from the nuclei (Srebrenik, 1973). The electrostatic potential is extracted from the wave function for the molecule using existing semiempirical or *ab initio* techniques and can be presented graphically. The single-point *ab initio* calculations (STO-3G) required to obtain and display electrostatic potentials for a molecule containing 20 non-hydrogen atoms can be performed, and graphically displayed, in approximately 1 h on a medium-sized workstation. Electrostatic potentials have been used to obtain two- or three-dimensional isopotential contours or surfaces, for predicting differences in electrophilicity, nucleophilicity, and binding interactions of biomolecules, and for exploring the role of charged groups on catalysis in proteases (Venanzi et al., 1992; Sjoberg & Politzer, 1990; Lamotte-Brasseur et al., 1990).

Reactant and Transition-State Structures. Kinetic isotope effects and the vibrational modeling for the transition state stabilized by nucleoside hydrolase have been previously reported (Horenstein et al., 1991). The truncated inosine used for vibrational analysis of the transition state was provided with the remaining atoms of inosine and with the partially bonded water nucleophile in the case of the transition-state structure. The structure used for inosine is the 3′-endo conformation as established by X-ray crystallography (Munns & Tollin, 1970) and as used in the vibrational analysis. Both the transition state and the product α-D-ribose were modeled in the 3′-exo conformation on the basis of the vibrational transition-state structure and least-motion principles. The hydroxyl group dihedrals were fixed equivalent to those employed for the transition-state calculations and were also varied at the transition state to determine the effect of hydroxyl placement. All bonds other than those defined by the vibrational analysis were minimized with Gaussian 92 using the STO-3G basis set (Frisch et al., 1992) in order to ensure that artifactual electronic effects due to bond-length deviations were not introduced. Electrostatic potentials were then calculated for the system by performing a single-point self-consistent-field calculation at the STO-3G level. The CUBE option of Gaussian 92 was used to sequentially extract electron density and electrostatic potential data. The results were visualized with the AVS-Chemistry viewer (Advanced Visual Systems Inc. and Molecular Simulations Inc.), allowing display of color-coded electrostatic potential data coincident with an electron density isosurface displayed at a density of 0.002 e/a_0^3 (Venanzi et al., 1992; Sjoberg & Politzer, 1990; Lamotte-Brasseur et al., 1990).

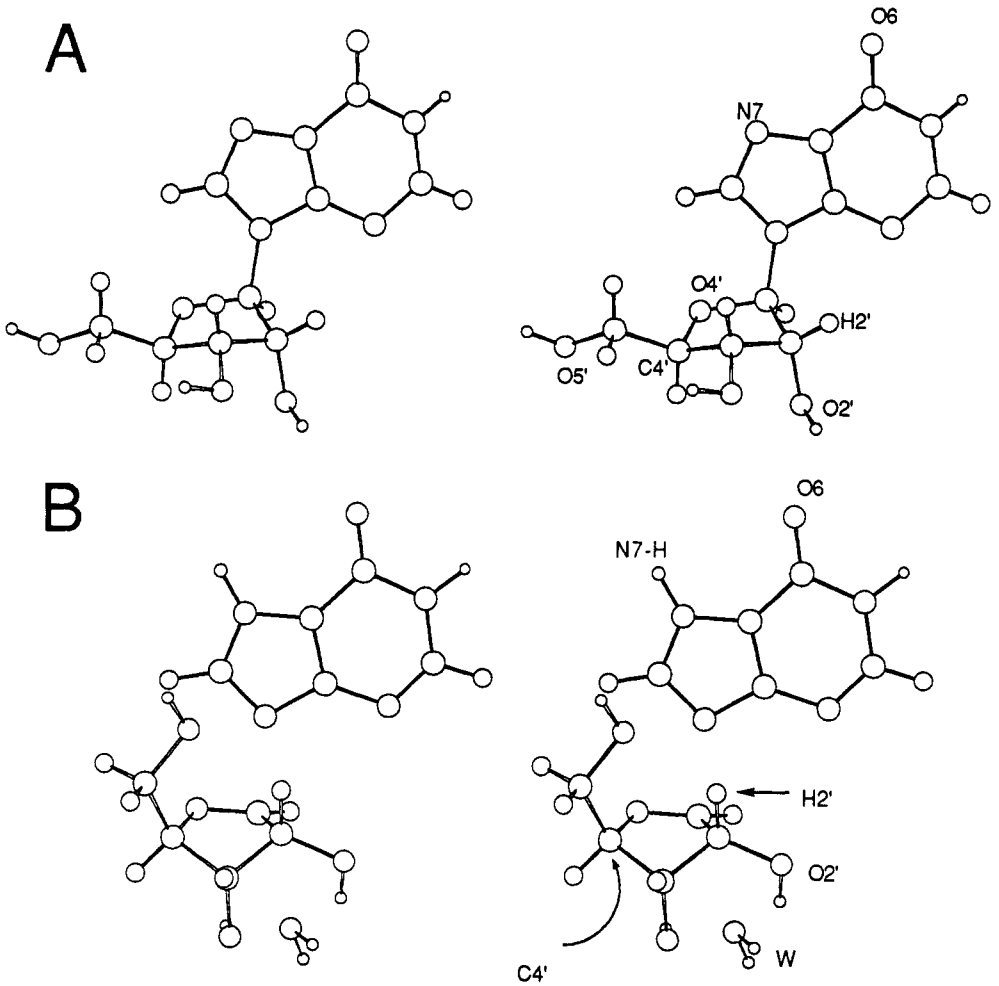

FIGURE 1: Stereoviews of the structure of inosine and the geometric transition-state model for hydrolysis of the N-glycosidic bond of inosine by nucleoside hydrolase. (A) The geometry for inosine is taken from the published crystal structure (Munns & Tollin, 1970). For the purpose of the electrostatic calculations, necessary hydrogens were added and all bonds minimized with the STO-3G basis set in Gaussian 92. The same treatment was applied to the transition-state structure, except for the coordinates of atoms defined by bond vibrational analysis (Horenstein et al., 1991). (B) The transition state. The C1′–N9 bond has increased from 1.49 to 2.0 Å, and the incipient water nucleophile has an oxygen–C1′ bond distance of approximately 3 Å. Note the protonation of N7 and the 3′-exo conformation of the ribosyl ring at the transition state.

Selection of Basis Set. The qualitative results reported here were insensitive to the choice of basis set used for the calculation of the molecular electrostatic potentials. Although the absolute value of the calculated molecular electrostatic potentials varied with basis set, the location of regions of low and high electrostatic potential varied little between STO-3G and 6-31G basis sets.

RESULTS AND DISCUSSION

Geometric Features of the Transition State. Key features used to construct the transition-state model of Figure 1 include the C3′-exo ribosyl ring conformation, required by the near planarity about C1′–O4′ and the overlap of the H2′–C2′ bond with the developing p orbital at C1′. The conformation of the hydroxymethyl group is dictated by the unusual kinetic isotope effect of 1.051 measured at H5′ using [5′-^{3}H]inosine (Horenstein et al., 1991). This normal isotope effect arises from a net decrease in the magnitude of the force constants involving H5′. This could be achieved by a small distortion at C5′ toward planarity. Inspection of molecular models indicates that the mechanics of flattening at C5′ and maintaining a C3′-exo ribosyl ring conformation can only be simultaneously satisfied by placing the hydroxymethyl group in the conformation shown in Figure 1. The C–N glycosidic bond is nearly cleaved with a length near 2.0 Å while the attacking water oxygen nucleophile is located 3 Å from C1′, poised to trap the ribosyl moiety. The hypoxanthine leaving group is protonated at N7, distal from the glycosidic linkage.[1] This feature of the transition state is required by the value of the kinetic isotope effect observed with [9-^{15}N]inosine, the lack of substrate activity for 7-deazaadenosine, and the solvent deuterium isotope effects (Parkin et al., 1991b; Horenstein et al., 1991). The low overall bond order to the ribosyl ring requires that it bear a substantial positive charge. The transition state has a complex structure because of multiple bond interactions at C1′–O4′, the site from which the electron deficiency originates. Partial bonding of the ribosyl residue to the departing hypoxanthine and the association of ribose with the attacking water nucleophile make it difficult to provide a simple description of charge distribution. The electronic properties of the transition state were investigated using the molecular electrostatic potential calculations described in Methods.

[1] A low-energy barrier hydrogen bond to N7 could serve the same role as protonation. Qualitatively, this would also be consistent with the observed 9-^{15}N isotope effects. We note that such hydrogen bonds would afford solvent deuterium isotope effects on the order of 0.4, while the observed solvent deuterium isotope effect is 1.30 (Horenstein et al., 1991). The possibility remains that one or more counterbalancing proton transfers occur, to produce the experimentally observed value. We thank a reviewer for pointing out this possibility.

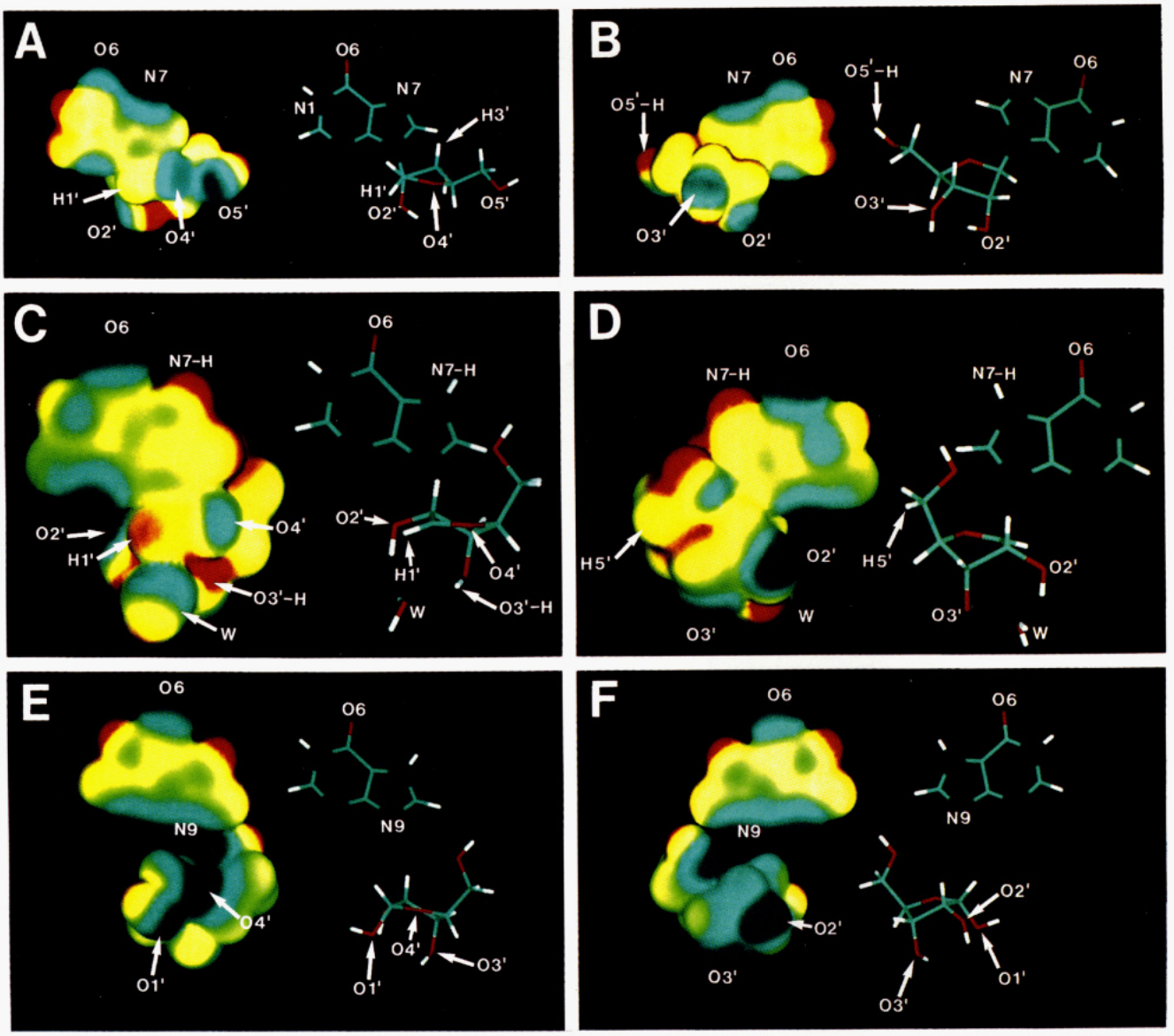

FIGURE 2: Electrostatic potential surfaces for free inosine, inosine at the transition state, and products ribose and hypoxanthine. The stick figures to the right in each panel are shown in the same orientation as the electrostatic potential surfaces. The blue regions are the most negative potentials and the red the most positive on the electrostatic potential surfaces (left figure in each panel). The energy difference from blue to red regions is approximately 63 kcal/mol (electrostatic potential × unit charge). Red regions represent areas most likely to interact with electron-rich enzymatic groups or benefit from stabilizing dipolar interactions. The surfaces are displayed at a value of electron density equal to 0.002 e/a_0^3, encompassing greater than 95% of the electron density (Sjoberg & Politzer, 1990). Each stick and surface pair (A–B, C–D, and E–F) represents the front and back views of the same structure. (A and B) Electrostatic potential surfaces for inosine. Hydrogens on N1, O2′, O3′, and O5′ have a highly positive electrostatic potential, illustrating the electrostatic basis for their utility as hydrogen bond donors. Unprotonated heteroatoms N3, N7, O6, and O4′ have negative electrostatic potential as expected for hydrogen bond acceptors. (C and D) Electrostatic potential surfaces for the transition state. Note the substantial positive potential at C1′–H1′ and the loss of negative potential for the ribosyl O4′, relative to O4′ of inosine. This decreased negative potential is consistent with its electron donation to the developing electron deficiency centered at C1′. (E and F) Electrostatic potential surfaces for the products ribose and hypoxanthine prior to release from the enzyme. The ribosyl configuration and the hypoxanthine protonation pattern imposed at the transition state are proposed to remain at this point in the reaction coordinate. Note the extensive redistribution of electrostatic potential. In particular, the strongly negative potential in the region of the former glycosidic linkage provides a repulsive force between the ribose and hypoxanthine molecules.

Electronic Nature of Inosine, the Transition State, and Products. The electrostatic potential surface for inosine is shown in Figure 2A,B. Lone pairs on nitrogen (N3 and N7) and oxygens of the purine (O6) and the ribose ring oxygen (O4′) have the most negative electrostatic potentials (blue, in Figure 2A,B). Hydrogen atoms bound to oxygen and nitrogen are the most positive regions of reactant-state inosine (red, in Figure 2A,B) in accord with the polar nature of these bonds (Siggel et al., 1988). The electrostatic potential surface provides an easily recognized pattern of sites which can accept or donate hydrogen bonds (blue and red regions, respectively, of Figure 2A,B). These interactions plus the hydrophobic nature of the planar purine ring are the forces which stabilize the Michaelis complex of nucleoside hydrolase and inosine since no groups with pK_a values between 4.5 and 9.5 are involved in substrate binding (Parkin et al., 1991b).

The electrostatic potential surface for the transition state stabilized by nucleoside hydrolase has a highly modified surface charge relative to substrate (Figure 2, compare panels A and B with panels C and D). Unique features of the transition state include an accumulation of positive charge in both the ribose ring and the imidazole portion of the departing hypoxanthine ring. The positive charge is not intensely concentrated around C1′–O4′ since the partial bond order, approximately 0.2, remaining between the hypoxanthine ring and the ribosyl residue allows some of the charge to reside in

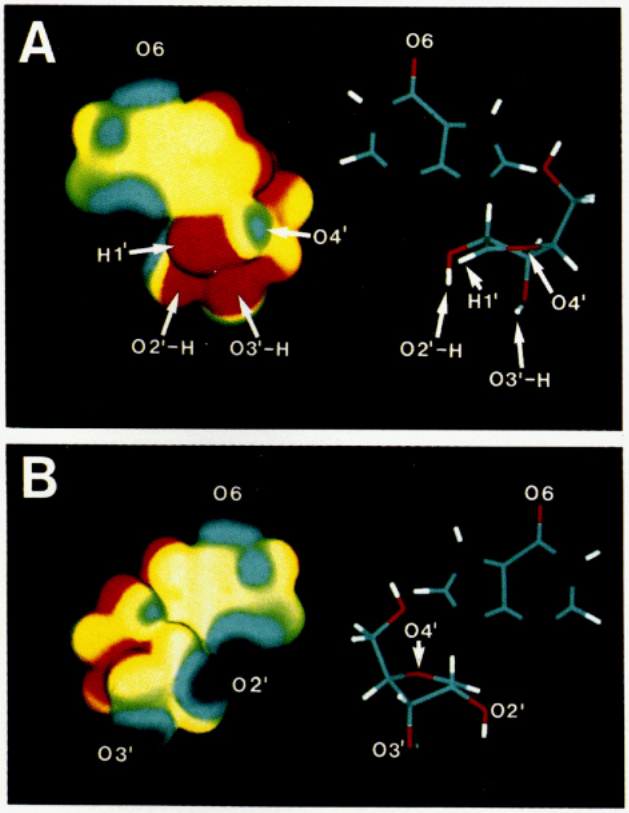

FIGURE 3: Electrostatic potential surfaces for the transition state with the attacking water nucleophile removed. Panels A and B provide two views of the same structure. The same energy levels are used to display this figure as in Figure 2C,D. Comparison with Figure 2C demonstrates the moderating effect of the attacking water on the electrostatic potential at C1′–H1′ of the transition state.

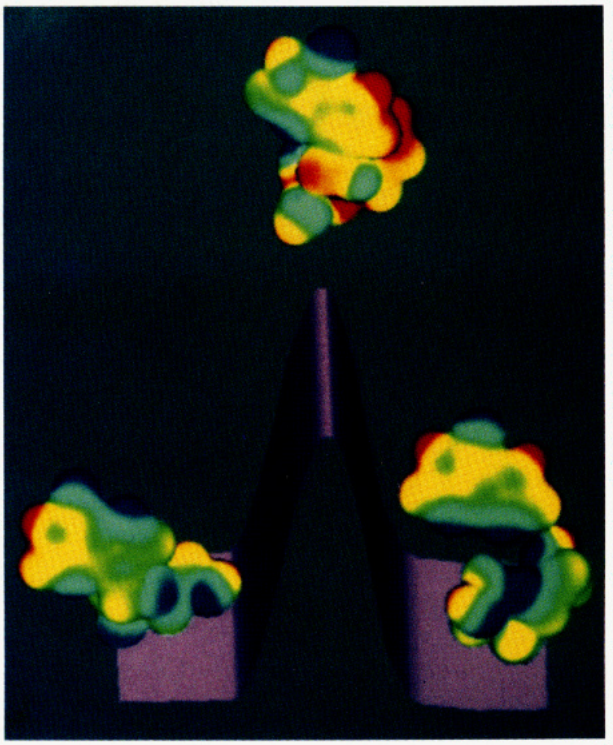

FIGURE 4: Reaction coordinate diagram for the hydrolysis of inosine by nucleoside hydrolase. On the left is the molecular electrostatic potential surface of inosine prior to interaction with the enzyme. At the top of the reaction coordinate diagram, the transition-state structure shows substantial changes in charge and geometry from reactant inosine. The structure on the lower right is the enzyme-bound ribose and hypoxanthine prior to their release into bulk solvent. The structures correspond to those in Figure 2, panels A, C, and E.

the hypoxanthine ring, particularly around C8. The N7 hydrogen displays a positive electrostatic potential due to the high polarity of the N–H bond. The bottom face of the ribosyl ring is not positive. The attacking water nucleophile, though just outside of bonding distance at approximately 3 Å, is used to stabilize the charge development at C1′ through its nonbonding electrons. Solvent reactivity studies have shown that this is a specific H_2O, attacking from an enzyme-directed site which exludes methanol (Parkin et al., 1991b). In the absence of the attacking water, the bottom face of the ribose residue is highly positive (Figure 3). Banait and Jencks (1991) have proposed that the intimate association of solvent with developing glycosyl cations is required for their (transient) formation. These calculations provide a qualitative demonstration of the diminution of electrostatic potential resulting from the association of the water nucleophile. The results also agree with previous theoretical studies of riboside hydrolysis that employed net atomic charges. Calculations for both purine[2] and nicotinamide riboside transition states indicate that the charge is delocalized across the ribosyl residue, water, and leaving group and is distributed as a function of the position of the transition state on the reaction coordinate [e.g., Schroder et al. (1992)].

The electrostatic potential of the products (Figure 2E,F) shows a substantial increase in electron density in the region previously occupied by the glycosidic linkage and a loss of positive electrostatic potential in the hypoxanthine ring. The strongly negative electrostatic potential in this region causes hypoxanthine–ribose repulsion and will facilitate diffusion of the products from the active site. The high K_i of 25 mM observed for hypoxanthine in the presence of ribose is consistent with this repulsion (Parkin et al., 1991b). As the reaction proceeds from bound inosine through the transition state and to products, substantial changes in the electrostatic potential occur.

Molecular Electrostatic Changes through the Reaction Coordinate. The results of Figure 2 are summarized in a schematic reaction coordinate diagram for nucleoside hydrolase (Figure 4). The rate enhancement imposed by nucleoside hydrolase is similar to that for AMP nucleosidase, which has been estimated to be 6×10^{12} that of the noncatalyzed reaction under similar conditions (DeWolf et al., 1979). These changes are in accord with the proposals that enzymes facilitate changes in electrostatic energy during catalysis (Warshel et al., 1989; Warshel, 1991). Charges which develop at the transition state of nucleoside hydrolase are distributed over several atoms and are strongly influenced by the attacking water molecule and by transition-state geometry. The common portrait for oxycarbonium structures with charge residing on one or two atoms in a resonance structure is thus an oversimplification of transition states which are rich in adjacent groups.

Effects of Conformation on Molecular Electrostatic Potential. Information on the rotational conformations about the C–O bonds of individual ribose hydroxyl groups is not available from the analysis of kinetic isotope effects. Remote conformational changes are not detected in kinetic isotope effect experiments or bond-vibrational analysis unless they cause changes in vibrational force constants (Stern &

[2] Horenstein and Schramm, unpublished results. Summation of net atomic charges over the ribosyl and hypoxanthine rings, respectively, allowed estimation of the charge partitioning between the two residues. These results compare favorably to those of Schroder et al. (1992).

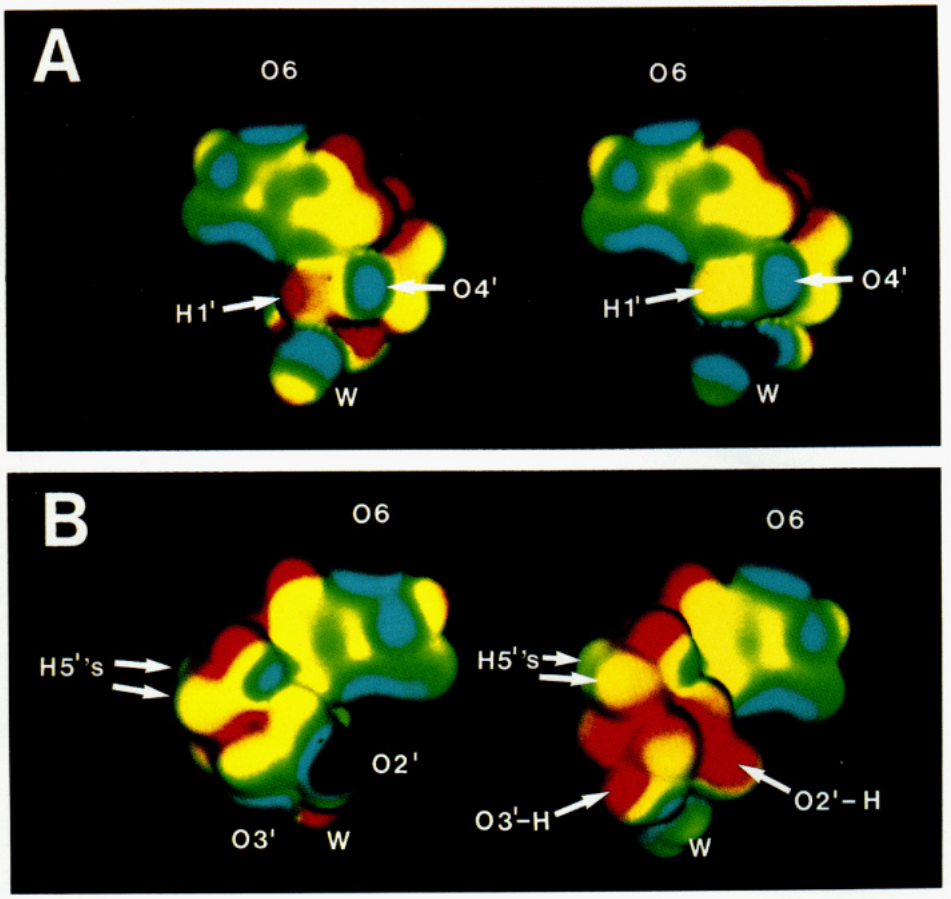

FIGURE 5: Effect of hydroxyl group rotomeric conformation on the electrostatic potential surface of the transition state. Panels A and B show front and rear views of the transition state. The structures on the left in panels A and B correspond to panels C and D of Figure 2, with the hydroxyl rotomeric conformation shown in Figure 6, upper stereo pair. The structures on the right in panels A and B show the effect of rotating the hydroxyl hydrogens to the position shown in Figure 6, lower stereo pair. The same energy levels are used for the display as in Figure 2. Comparison with Figure 2 demonstrates that the electrostatic potential surface of the transition state is sensitive to conformational effects. Loss of positive electrostatic potential from the C1′–O4′ region (panel A, left) to the "back" face of the ribosyl ring (panel B, right) occurs by assuming hydroxyl rotomers that point nonbonding hydroxyl electrons toward the C1′–O4′ bond.

Wolfsberg, 1966). Electrostatic potential calculations can provide insight into transition-state geometry by analyzing the electronic effects of the conformation of the O2′, O3′, and O5′ hydroxyl groups as they are rotated about the C–O bond. During rotation, the hydroxyl lone pairs change their orientation with respect to the C1′–O4′ bond. Figure 2A is the reference conformation that results in localization of the positive electrostatic potential near C1′–O4′. The surface corresponding to this conformation is reproduced in the left structures in Figure 5A,B. Figure 5A,B, right structures, shows the effect of rotating the O2′, O3′, and O5′ dihedrals such that the O2′–H bond is anti to the C1′–C2′ bond, the O3′–H bond is anti to the C3′–C2′ bond, and the O5′–H bond is anti to the C4′–C5′ bond. The orientation of the O2′–H and O3′–H hydroxyls for these calculations is illustrated in Figure 6. This set of rotations orients the hydroxyl dipoles to minimize the development of positive charge at C1′–O4′. With this configuration, the surface describing the electrostatic potential of the region at C1′–O4′ is altered substantially to redistribute transition-state charge. The positive electrostatic potential shifts into the center of the top face of the ribosyl ring. If the transition state were bound in the active site with the hydroxyls oriented as in Figure 5A,B, right structures (Figure 6, right structure), more electrostatic binding energy could be developed by placing a negatively charged group or suitable dipole over the ribose ring, rather than in the vicinity of C1′–O4′.

The surfaces shown in Figure 5 represent the extremes for the degree of positive electrostatic potential found at C1′–O4′. A systematic examination of the effect of the O2′, O3′, and O5′ dihedrals demonstrates that local substrate conformational effects can have a profound effect on the electronic nature of the transition state. Structural features of the transition state, sometimes *remote* from the site of bond breaking and forming, are likely to be used to distribute or localize charge development to optimize structures which can be stabilized at enzymatic transition states.

An example of these effects is provided by the relative stabilities of the N-glycosidic bonds of ribo- and deoxyribonucleosides. Ribofuranosides react 10^2–10^3-fold slower in acid-catalyzed hydrolysis than do the corresponding deoxyribofuranosides (Capon, 1969). This trend has not been observed for the corresponding enzymatic reactions. Although the 2′-deoxyribonucleosidases are poorly characterized, limited information suggests that the catalytic efficiency for deoxyribonucleosidases is several orders of magnitude less than for nucleosidases (Steenkamp, 1991; Miller et al., 1984). This evidence suggests that ribofuranosyl hydrolysis involves precise positioning of hydroxyl groups to counteract destabilization of the transition state by the inductive effect of the 2′-hydroxyl. A related suggestion has been made for hydrolysis of nicotinamide ribosides in which the 2′-hydroxyl may be deprotonated or involved in strong hydrogen bond donation (Johnson et al., 1988). Another example of electronic participation of the 2′-hydroxyl in catalysis is the nucleophilic

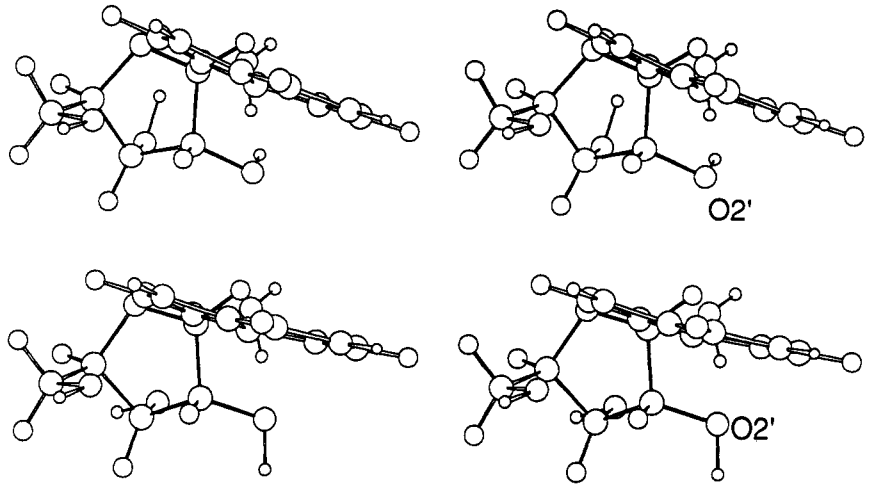

FIGURE 6: Comparison of hydroxyl group rotomers for transition-state structures. The rotomeric conformation shown in the top stereoview is used in Figure 2C,D and in Figure 5A,B, left structures. The configuration shown in the bottom stereoview is used in Figure 5A,B, right structures. The view is from above the plane of the ribose ring. For reference, O2′ has been labeled in each structure.

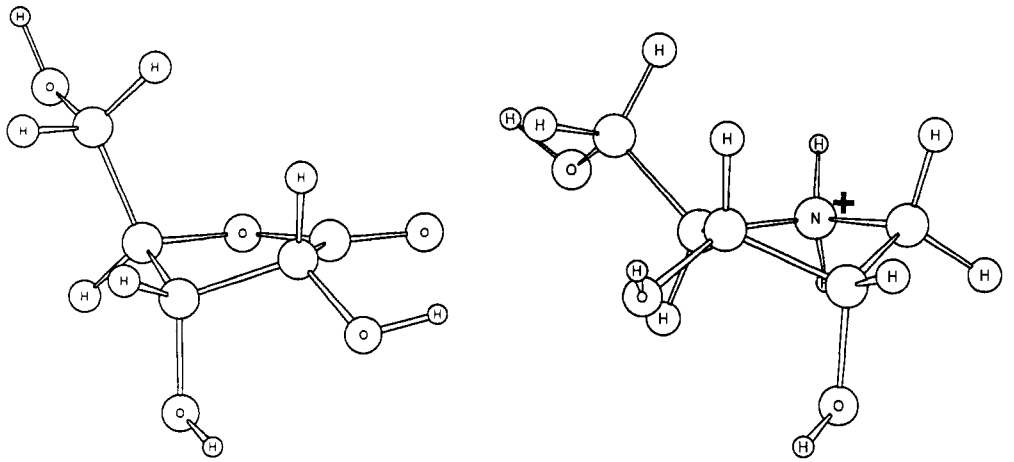

FIGURE 7: Transition-state analogues for nucleoside hydrolase. The left structure, ribonolactone, is a geometric transition-state analogue by virtue of its 3-exo ring configuration. The structure on the right is the protonated form of 1,4-dideoxy-1,4-iminoribitol, an electronic transition-state analogue.

behavior of this group in catalytic RNA (Cech et al., 1992).

Environmental Effects on the Molecular Electrostatic Potential. The effects of hydroxyl rotation at the transition state demonstrate that electrostatic potential can be perturbed by conformational effects imposed by enzymic groups. It is possible that additional perturbations could arise from the amino acid side chains interacting with the transition state or differences in solvation along the reaction coordinate. The molecular electrostatic potentials presented in Figures 2–5 represent molecules *in vacuo*, unperturbed by contributions from the solvent or protein.[3] This approximation is reasonable for qualitative comparison of the *differences* between reactant, enzyme-bound conformations of the transition state, and products and for examining local changes in rotomer composition of the transition state. With detailed knowledge of the active site residues at the transition state, it would be possible to evaluate the role of polarization on the calculated molecular electrostatic potential (Weinstein et al., 1981). Recently, Lockhart and Kim (1992) reported experimental measurement of the field associated with the α-helix dipole of model peptides, finding a value of 10^7 V/cm. The electrostatic potential for the transition-state model was calculated in the presence of applied fields of 10^8 V/cm in various orientations. No qualitative changes in location of regions of high and low electrostatic potential were observed. However, electric field strengths of 10^9 V/cm produced qualitative distortions of the electrostatic potential. Thus, the applied field strengths associated with protein structural features are unlikely to cause substantial distortion of the electrostatic potentials reported in Figure 2–5. Under special conditions, electric field effects approaching 10^9 V/cm may be possible in proteins (Naray-Szabo et al., 1987), but geometric and environmental uncertainties make it impractical to address this issue until protein structural data are available.

Electronic Nature of the Transition State. The transition-state calculations described in this work indicate that the electrostatic potential surface of the transition state for nucleoside hydrolase has unique electronic and geometric properties, which are not present in substrate or products. The surface of the transition state is plastic, and conformational features can be readily modified by enzyme-directed changes in the transition-state geometry. The archetypical transition

[3] The electrostatic potential calculations reported here do not consider the effects of solvent except for the partially bonded hydroxyl which is involved in transition-state formation. It has been reported that electron distributions of substituted heterocycles are significantly altered in aqueous solution (Cramer & Truhlar, 1992a,b). Since all calculations here are *in vacuo*, the exact electrostatic potentials may be altered but should provide a qualitative picture of relative change between substrate, transition state, and products. The authors are grateful to a reviewer for these comments.

state for glycosidases invokes the interaction of an active site carboxyl residue with the positively charged glycosyl transition state [e.g., Sinnott (1990)]. The electrostatic potential surfaces demonstrated here for the nucleoside hydrolase reaction indicate that the positive electrostatic potential is unlikely to be a highly localized charge at C1′–O4′. Conformations which reduce charge buildup at this position could be preferred, with little energy penalty for the associated conformational change. The results indicate that nucleoside hydrolase could provide electrostatic stabilization of glycosyl–cation transition states by interactions at sites other than at the "oxonium" group. The inability of nucleoside hydrolase to hydrolyze 2′-, 3′-, and 5′-deoxynucleosides supports this proposal (Parkin et al., 1991b). Ways to further address this question are through high-resolution X-ray crystallographic analysis of the active site and studies with transition-state analogue inhibitors. Studies using both approaches are underway.

Transition-State Structure as a Blueprint for Inhibitor Design. Nucleoside analogues with a range of substitutions in the purine or ribosyl rings are ineffective inhibitors of nucleoside hydrolase. A survey of such compounds gave weak competitive inhibition with K_i values ranging from 2 to 44 mM, compared to the K_d for inosine of 0.38 mM (Parkin et al., 1991b). The value of transition-state knowledge is apparent by considering a ribose analogue with partial features of the transition state. Ribonolactone (Figure 7A) has sp^2 hybridization at C1, the 3-exo configuration of the ribosyl ring, and is a competetive inhibitor with a K_i of 0.09 mM. An electronic transition-state analogue, 1,4-dideoxy-1,4-iminoribitol (Figure 7B) (Fleet et al., 1988) carries a positive charge at the nitrogen which replaces the C4 oxygen of ribitol. This compound is a more potent inhibitor of nucleoside hydrolase,[4] with a K_i of 0.01 mM. Inhibitors with additional features of the transition state are being prepared.

Conclusions. Electrostatic potential surface analysis of the substrate, transition state, and products of nucleoside hydrolase provides novel insights into the changing geometric and charge features a substrate experiences as it traverses the reaction coordinate. Unique features of the transition state are readily deduced. Knowledge of both the geometric and electronic features of the transition state provides novel insights into catalysis and a logical blueprint for the design of transition-state inhibitors. The methodology described could be applied to any system for which multiple kinetic isotope effects can be measured and interpreted. Molecular electrostatic potential modeling of transition-state structures is readily performed and offers unique information on transition-state properties. This information can complement information obtained on ground-state structures, such as crystallographic techniques. It should soon be possible to place well-characterized transition-state structures into the crystallographically derived active sites of enzymes, providing a unique opportunity to explore the interaction of the proteins with actual transition-state structures.

REFERENCES

Bader, R. F. W. (1985) *Acc. Chem. Res. 18*, 9.

Banait, N. S., & Jencks, W. P. (1991) *J. Am. Chem. Soc. 113*, 7951.

Besler, B. H., Merz, K. M., Jr., & Kollman, P. A. (1990) *J. Comput. Chem. 11*, 431.

Brown, S. B., Dewar, M. J. S., Ford, G. P., Nelson, D. J., & Rzepa, H. S. (1978) *J. Am. Chem. Soc. 100*, 7832.

Capon, B. (1969) *Chem. Rev. 69*, 407.

Cech, T. R., Herschlag, D., Piccirilli, J. A., & Pyle, A. M. (1992) *J. Biol. Chem. 267*, 17479.

Cleland, W. W. (1982) *CRC Crit. Rev. Biochem. 13*, 385.

Cramer, C. J., & Truhlar, D. G. (1992a) *Chem. Phys. Lett. 198*, 74.

Cramer, C. J., & Truhlar, D. G. (1992b) *J. Comput.-Aided Mol. Des. 6*, 629.

DeWolf, W. E., Jr., Fullin, F. A., & Schramm, V. L. (1979) *J. Biol. Chem. 254*, 10868.

Fleet, G. W. J., & Son, J. C. (1988) *Tetrahedron 44*, 2637.

Frisch, M. J., Trucks, G. W., Head-Gordon, M., Gill, P. M. W., Wong, M. W., Foresman, J. B., Johnson, B. G., Schlegel, H. B., Robb, M. A., Replogle, E. S., Gomperts, R., Andres, J. L., Raghavachari, K., Binkley, J. S., Gonzalez, C., Martin, R. L., Fox, D. J., DeFrees, D. J., Baker, J., Stewart, J. J. P., & Pople, J. A. (1992) *Gaussian 92, Revision A*, Gaussian, Inc., Pittsburgh, PA.

Hackney, D. D. (1990) in *The Enzymes* (Sigman, D. S., & Boyer, P. D., Eds.) Vol. 19, p 1, Academic Press, San Diego.

Hammett, L. P. (1970) in *Physical Organic Chemistry*, 2nd ed., McGraw-Hill, New York.

Hermes, J. D., Morrical, S. W., O'Leary, M. H., & Cleland, W. W. (1984) *Biochemistry 23*, 5479.

Horenstein, B. A., Parkin, D. W., Estupinan, B., & Schramm, V. L. (1991) *Biochemistry 30*, 10788.

Huskey, W. P. (1991) in *Enzyme Mechanism from Isotope Effects* (Cook, P. F., Ed.) p 37, CRC Press, Boca Raton, FL.

Jencks, W. P. (1969) *Catalysis in Chemistry and Enzymology*, McGraw-Hill, New York.

Johnson, R. W., Marschner, T. M., & Oppenheimer, N. J. (1988) *J. Am. Chem. Soc. 110*, 2257.

Knowles, J. R. (1991) *Nature 350*, 121.

Lamotte-Brasseur, J., Dive, G., Dehareng, D., & Ghuysen, J.-M. (1990) *J. Theor. Biol. 145*, 183.

Lerner, R. A., Benkovic, S. J., & Schultz, P. G. (1991) *Science 252*, 659.

Lockhart, D. J., & Kim, P. S. (1992) *Science 257*, 5072.

Lu, D.-H., Maurice, D., & Truhlar, D. G. (1990) *J. Am. Chem. Soc. 112*, 6206.

Markham, G. D., Parkin, D. W., Mentch, F., & Schramm, V. L. (1987) *J. Biol. Chem. 262*, 5609.

McClennan, D. J. (1987) in *Isotopes in Organic Chemistry* (Buncel, E., & Lee, C. C., Eds.) Chapter 7, Elsevier, New York.

Menger, F. M. (1992) *Biochemistry 31*, 5368.

Mentch, F., Parkin, D. W., & Schramm, V. L. (1987) *Biochemistry 26*, 921.

Miller, R. L., Sabourin, C. L. K., Krenetsky, T. A., Berens, R. L., & Marr, J. J. (1984) *J. Biol. Chem. 259*, 5073.

Munns, A. R. I., & Tollin, P. (1970) *Acta Crystallogr., Sect. B 26*, 1101.

Naray-Szabo, G., Surjan, P. R., & Angyan, J. G. (1987) in *Applied Quantum Chemistry*, p 249, D. Reidel Publishing Co., Dordrecht, Holland.

Parkin, D. W., & Schramm, V. L. (1987) *Biochemistry 26*, 913.

Parkin, D. W., Mentch, F., Banks, G. A., Horenstein, B. A., & Schramm, V. L. (1991a) *Biochemistry 30*, 4586.

Parkin, D. W., Horenstein, B. A., Abdulah, D. R., Estupinan, B., & Schramm, V. L. (1991b) *J. Biol. Chem. 266*, 20658.

Perigaud, C., Gosselin, G., & Imbach, J.-L. (1992) *Nucleosides Nucleotides 11*, 903.

Politzer, P., & Truhlar, D. G., Eds. (1981) *Chemical Applications of Atomic and Molecular Electrostatic Potentials*, Plenum Press, New York.

Rodgers, J., Femec, D. A., & Schowen, R. L. (1982) *J. Am. Chem. Soc. 104*, 3263.

Saunders, M., Laidig, K. E., & Wolfsberg, M. (1989) *J. Am. Chem. Soc. 111*, 8989.

[4] Horenstein and Schramm, manuscript submitted for publication.

Schroder, S., Buckley, N., Oppenheimer, N. J., & Kollman, P. A. (1992) *J. Am. Chem. Soc. 114*, 8232.
Siggel, M. R. F., Streitweiser, A., Jr., & Thomas, T. D. (1988) *J. Am. Chem. Soc. 110*, 8022.
Sims, L. B., & Lewis, D. E. (1984) in *Isotopes in Organic Chemistry* (Buncel, E., & Lee, C. C., Eds.) p 161, Elsevier, New York.
Sinnott, M. L. (1990) *Chem. Rev. 90*, 1171.
Sjoberg, P., & Politzer, P. (1990) *J. Phys. Chem. 94*, 3959.
Srebrenik, S., Weinstein, H., & Pauncz, R. (1973) *Chem. Phys. Lett. 20*, 419.
Steenkamp, D. J. (1991) *Eur. J. Biochem. 197*, 431.
Stern, M. J., & Wolfsberg, M. (1966) *J. Chem. Phys. 45*, 2618.
Suhnel, J., & Schowen, R. L. (1991) in *Enzyme Mechanism from Isotope Effects* (Cook, P. F., Ed.) p 3, CRC Press, Boca Raton, FL.
Venanzi, C. A., Planr, C., & Venanzi, T. J. (1992) *J. Med. Chem. 35*, 1643.
Warshel, A. (1991) *Computer Modeling of Chemical Reactions in Enzymes and Solutions*, Chapter 9, John Wiley & Sons, New York.
Warshel, A., Naray-Szabo, G., Sussman, F., & Hwang, J.-K. (1989) *Biochemistry 28*, 3629.
Weinstein, H., Osman, R., Green, J. P., & Tipiol, S. (1981) in *Chemical Applications of Atomic and Molecular Electrostatic Potentials* (Politzer, P., & Truhlar, D. G., Eds.) p 309, Plenum Press, New York.
Williams, A. (1992) *Adv. Phys. Org. Chem. 27*, 1.